Electronic Supplementary Material (ESI) for Physical Chemistry Chemical Physics.

SUPPLEMENTARY INFORMATION

Plasmon Resonances Tailored by Fano Profiles in Silver-Based Core-Shell Nanoparticles

Michel Pellarin, Michel Broyer, Jean Lermé, Marie-Ange Lebeault, Julien Ramade, and Emmanuel Cottancin*

Institut Lumière Matière, UMR5306 Université Lyon 1-CNRS, Université de Lyon, 69622 Villeurbanne Cedex, France

1. Effective dielectric functions of coinage metals: introduction of interband transitions.

Dimensionless dielectric functions of coinage metals are chosen to be parameterized in the form:

$$\varepsilon(\omega) = 1 - \frac{\omega_p^2}{\omega(\omega + i\Gamma)} + \chi_{IB}(\omega) \qquad \text{(SI1)}$$

, where the dielectric susceptibility $\chi_{IB}(\omega)$ (real and imaginary parts) associated to IB transitions is extracted from a mathematical processing. $\chi_{IB}(\omega) = \varepsilon_{IB}(\omega) - 1$ can be actually evaluated from tabulated experimental values of the total dielectric function $\varepsilon^{exp}(\omega)$ by extracting $Im(\chi_{IB}(\omega))$ from the difference between the imaginary part $Im(\varepsilon^{exp}(\omega))$ and the best fit of a Drude term $Im(\varepsilon_F(\omega))$ assuming a threshold ω_{IB} below which $Im(\chi_{IB}(\omega)) = 0$. Afterwards $Re(\chi_{IB}(\omega))$ is obtained from $Im(\chi_{IB}(\omega))$ by a Kramers-Kronig analysis (see Figure SI1).[1-2]

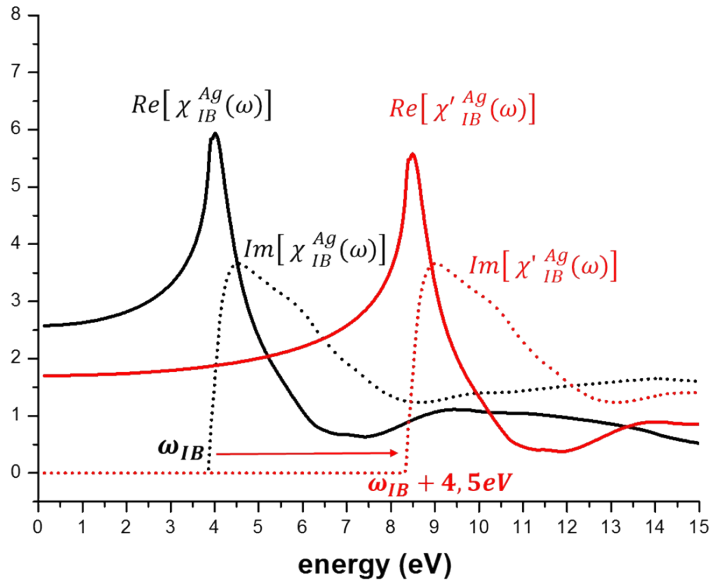

Figure SI1: Real and imaginary parts of the dielectric susceptibility associated to IB transitions and core polarization in silver. Black and red curves are constructed from experimental tables [3] without or with an artificial shift of 4.5eV of the IB threshold respectively.

Parameters in formula (SI1) are adjusted so as to obtain the best compromise ensuring the reproducing of the experimental dielectric functions (Fig. SI2) and the plasmon spectra of small nanoparticles (Fig. SI3a). Formula (SI1) can also be adapted to account for the dielectric screening by the ionic background ignoring energy dissipation through IB transition excitations ($Im\left[\chi_{IB}^{Ag}(\omega)\right]$=0 and $1+Re\left[\chi_{IB}^{Ag}(\omega)\right]=\varepsilon_\infty=cst$). Adjusted ε_∞values are also given in Table SI1.

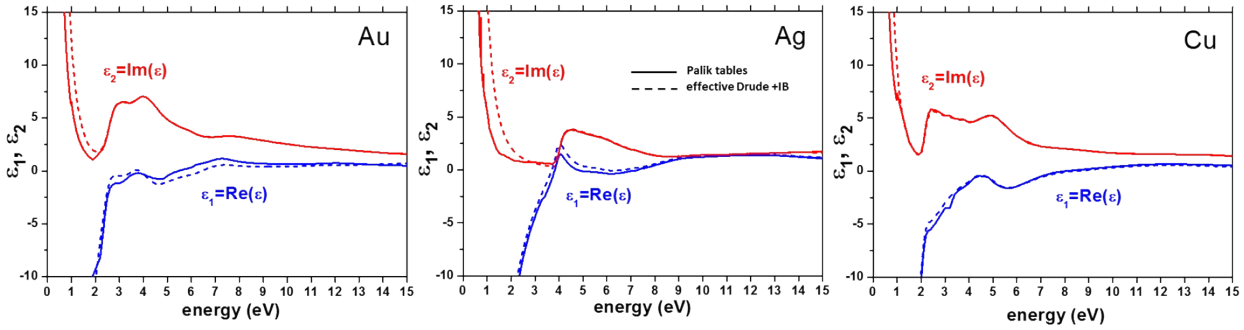

Figure SI2. Comparison between experimental [3] (full lines) and parameterized dielectric functions (dashed lines) for gold, silver and copper.

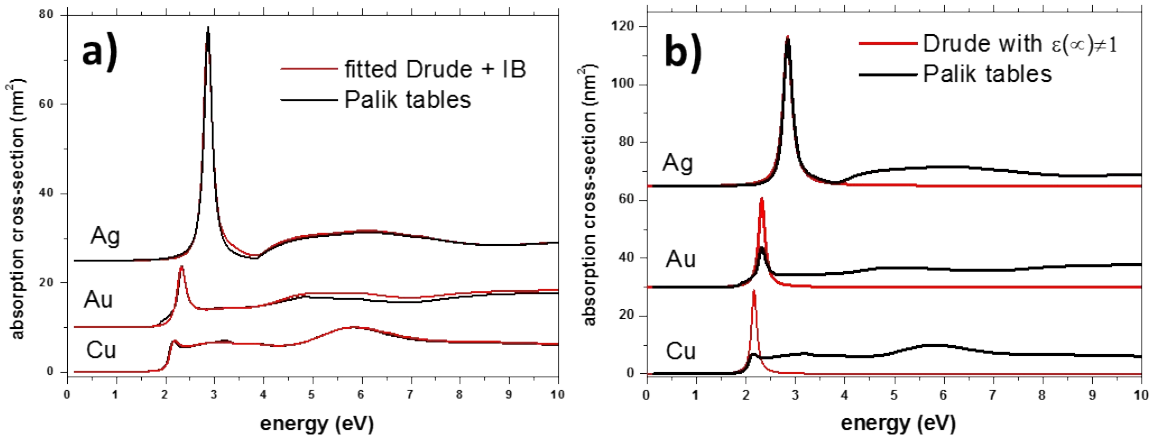

Figure SI3. (a) Comparison between absorption spectra of Ag, Au and Cu spheres (5nm in diameter) calculated within the Mie theory from experimental tabulated dielectric functions [3] (black curves) or from effective dielectric functions obtained by adding fitted Drude and interband contributions (red curves) (b) Comparison between absorption spectra of Ag, Au and Cu spheres (5nm in diameter) calculated within the Mie theory from experimental tabulated dielectric functions [3] (black curves) or from Drude–like dielectric functions with parameters (

ω_p, Γ, and ε_∞ *in Table SI1).* ε_∞ *is adjusted so as to reproduce the resonance energies at best (red curves)*

	ω_p (eV)	Γ (eV)	ε_∞	ω_{IB} (eV)
gold	9.1	0.15	10	2.05
silver	8.85	0.215	4.2	3.9
copper	8.85	0.125	11.5	1.95

Table SI1: Selected values of Drude parameters (volume plasmon energy ω_p*, damping rate* Γ*, high frequency limit dielectric constant* ε_∞*) and interband transition threshold (*ω_{IB}*) energy for gold, silver and copper.*

2 LSPR of single nanospheres and nanoshells

If the bulk dielectric function $\varepsilon(\omega)$ is chosen to describe the optical response of small clusters, the induced dipole $\vec{p}$ of a spherical particle with radius R (R<<c/ω) embedded in a medium of constant dielectric function ε_m and subject to an applied electric field $\vec{E}_0$ is defined by

$\vec{p} = \varepsilon_0 \alpha^S(\omega) \vec{E}_{0\,\varepsilon_m}$ (ε_0 is the dielectric constant of vacuum)

, where ε_0 is the dielectric constant of vacuum and $\alpha^S(\omega)$ the dynamical polarizability that writes

$$\alpha^S(\omega) = 3\left(\frac{4}{3}\pi R^3\right)\frac{(\varepsilon(\omega)-\varepsilon_m)}{(\varepsilon(\omega)+2\varepsilon_m)}$$

The derived absorption cross-section is

$$\sigma_{abs}^S(\omega) = k\,\mathrm{Im}\left[\alpha^S(\omega)\right] = \frac{9\omega\,\varepsilon_m^{3/2}}{c}\left(\frac{4}{3}\pi R^3\right)\frac{\varepsilon_2(\omega)}{(\varepsilon_1(\omega)+2\varepsilon_m)^2+\varepsilon_2(\omega)^2} \qquad \text{(SI3)}$$

, where $\varepsilon(\omega)$ is the dielectric function given by (SI1) and $\varepsilon_1(\omega)$ and $\varepsilon_2(\omega)$ its real and

imaginary parts respectively. $k = \frac{2\pi}{\lambda}\sqrt{\varepsilon_m} = \frac{\omega}{c}\sqrt{\varepsilon_m}$ is the wave vector in the outer medium.

$$\varepsilon_1(\omega) = 1 - \frac{\omega_p^2}{\left(\omega^2 + \Gamma^2\right)} + Re\left[\chi_{IB}(\omega)\right]$$

, and

$$\varepsilon_2(\omega) = \frac{\omega_p^2 \Gamma}{\omega\left(\omega^2 + \Gamma^2\right)} + Im\left[\chi_{IB}(\omega)\right]$$

We can define the interband contribution to the dielectric function as $\varepsilon_{IB}(\omega) = 1 + \chi_{IB}(\omega)$.

Since the numerator $\omega\varepsilon_2(\omega)$ in (SI3) varies slowly, the absorption cross-section $\sigma_{abs}^{S}(\omega)$ is maximum if the denominator

$$\left(\varepsilon_1(\omega) + 2\varepsilon_m\right)^2 + \varepsilon_2(\omega)^2 = \left(1 - \frac{\omega_p^2}{\omega^2 + \Gamma^2} + Re\left[\chi_{IB}(\omega)\right] + \right)^2 + \left(\frac{\omega_p^2 \Gamma}{\omega\left(\omega^2 + \Gamma^2\right)} + Im\left[\chi_{IB}(\omega)\right]\right)^2 \quad 2\varepsilon_m$$

(SI4)

is minimum.

This holds for

$$\omega_R^S = \frac{\omega_p}{\sqrt{Re\left[\varepsilon_{IB}\left(\omega_R^S\right)\right] + 2\varepsilon_m}}, \qquad \text{(SI5)}$$

when $Im\left[\chi_{IB}\left(\omega_R^S\right)\right] \cong 0 \; and \; \Gamma \ll \omega_R^S$.

In the absence of IB transitions (pure Drude metal) the dipolar resonance frequency becomes

$$\omega_R^S = \frac{\omega_p}{\sqrt{1 + 2\varepsilon_m}} \qquad \text{(SI6)}$$

If a dielectric spherical void (hole) of radius R and dielectric constant ε_m in an infinite metallic outer medium is considered instead of a spherical metallic particle embedded in an infinite dielectric medium of the same dielectric constant ε_m, the polarizabilty writes

$\alpha(\omega) = -3(\frac{4}{3}\pi R^3)\frac{(\varepsilon(\omega)-\varepsilon_m)}{(2\varepsilon(\omega)+\varepsilon_m)}$ and the resonance frequency under the same assumptions is

$$\omega_R^h = \frac{\omega_p}{\sqrt{1+\frac{\varepsilon_m}{2}}} \qquad \text{(SI7)}$$

The polarizability of a nanoshell (inner radius r_{in} and outer radius r_{out}, dielectric function $\varepsilon(\omega)$) embedded in a dielectric medium of dielectric function ε_m and enclosing a core of dielectric function ε_1 writes [4]

$$\alpha(\omega) = 3(\frac{4}{3}\pi r_{out}^3)\frac{(\varepsilon(\omega)-\varepsilon_m)(\varepsilon_1+2\varepsilon(\omega))+f(\varepsilon_1-\varepsilon(\omega))(\varepsilon_m+2\varepsilon(\omega))}{(\varepsilon(\omega)+2\varepsilon_m)(\varepsilon_1+2\varepsilon(\omega))+f(2\varepsilon(\omega)-2\varepsilon_m)(\varepsilon_1-\varepsilon(\omega))}$$

with $f=(\frac{r_{in}}{r_{out}})^3$;

in the particular case where $\varepsilon_m = \varepsilon_1$, $\alpha(\omega)$ can be expressed in the form

$$\alpha^{NS}(\omega) = 3(\frac{4}{3}\pi r_{out}^3)\frac{(\varepsilon(\omega)-\varepsilon_a^+)(\varepsilon(\omega)-\varepsilon_a^-)}{(\varepsilon(\omega)-\varepsilon_b^+)(\varepsilon(\omega)-\varepsilon_b^-)}$$

, with $\varepsilon_a^{\pm} = \frac{1}{2}\left[-X_a \pm \sqrt{X_a^2+2\varepsilon_m^2}\right]$, $\varepsilon_b^{\pm} = \frac{1}{2}\left[-X_b \pm \sqrt{X_b^2-4\varepsilon_m^2}\right]$, $X_a = -\frac{\varepsilon_m}{2}$, and $X_b = \frac{\varepsilon_m 5+4f}{2\ \ 1-f}$

The corresponding absorption cross-section is

$$\sigma_{abs}^{NS}(\omega) = k\,\mathrm{Im}\left[\alpha^{NS}(\omega)\right] \qquad \text{(SI8)}$$

For a Drude-like metal ($Im[\chi_{IB}(\omega_R)] \cong 0$) and assuming $\Gamma \ll \omega_R$, the solutions for f<<1 are:

$$\omega_{\bar{R}} = \frac{\omega_p}{\sqrt{1+Re(\chi_{IB}(\omega_{\bar{R}})+2\varepsilon_1}} = \frac{\omega_p}{\sqrt{1+Re(\chi_{IB}(\omega_{\bar{R}})+2\varepsilon_m}} \qquad \text{(SI9)}$$

, and

$$\omega_R^+ = \frac{\omega_p}{\sqrt{1 + Re(\chi_{IB}(\omega_R^+) + \frac{\varepsilon_m}{2}}} \qquad \text{(SI10)}$$

They correspond to the limit resonances for the bare sphere and for the void respectively.

The solutions for f≈1 (infinitely thin shell) are:

$$\omega_R^- = \frac{\omega_p}{\sqrt{1 + Re(\chi_{IB}(\omega_R^-) + \frac{9}{2}\frac{\varepsilon_m}{(1-f)}}} \approx 0 \qquad \text{(SI11)}$$

, and

$$\omega_R^+ = \frac{\omega_p}{\sqrt{1 + Re(\chi_{IB}(\omega_R^+)}} \qquad \text{(SI12)}$$

3 Location of the LSPR versus the IB transition continuum threshold in silver nanospheres

Since the numerator in the nanosphere absorption cross-section ($\omega\varepsilon_2(\omega)$ in (SI3)) varies slowly around ω_R^S, the resonance condition can be approximately obtained by minimizing the denominator (SI4). This is studied graphically in Figure SI4 for various dielectric functions that differ from the tabulated dielectric function of silver by the offset value δ applied to the threshold of the IB absorption continnum (ω_{IB}). The principle is to define a shifted imaginary part of the dielectric susceptibility $Im[\chi_{IB}^{shifted}(\omega)]$ by assuming that ($Im[\chi_{IB}^{shifted}(\omega)] = Im[\chi_{IB}^{Ag}(\omega-\delta)]$). The real part $Re[\chi_{IB}^{shifted}(\omega)]$ differs from the real part of $\chi_{IB}^{Ag}(\omega)$ and is obtained from $Im[\chi_{IB}^{shifted}(\omega)]$ through a Kramers- Kronig analysis.

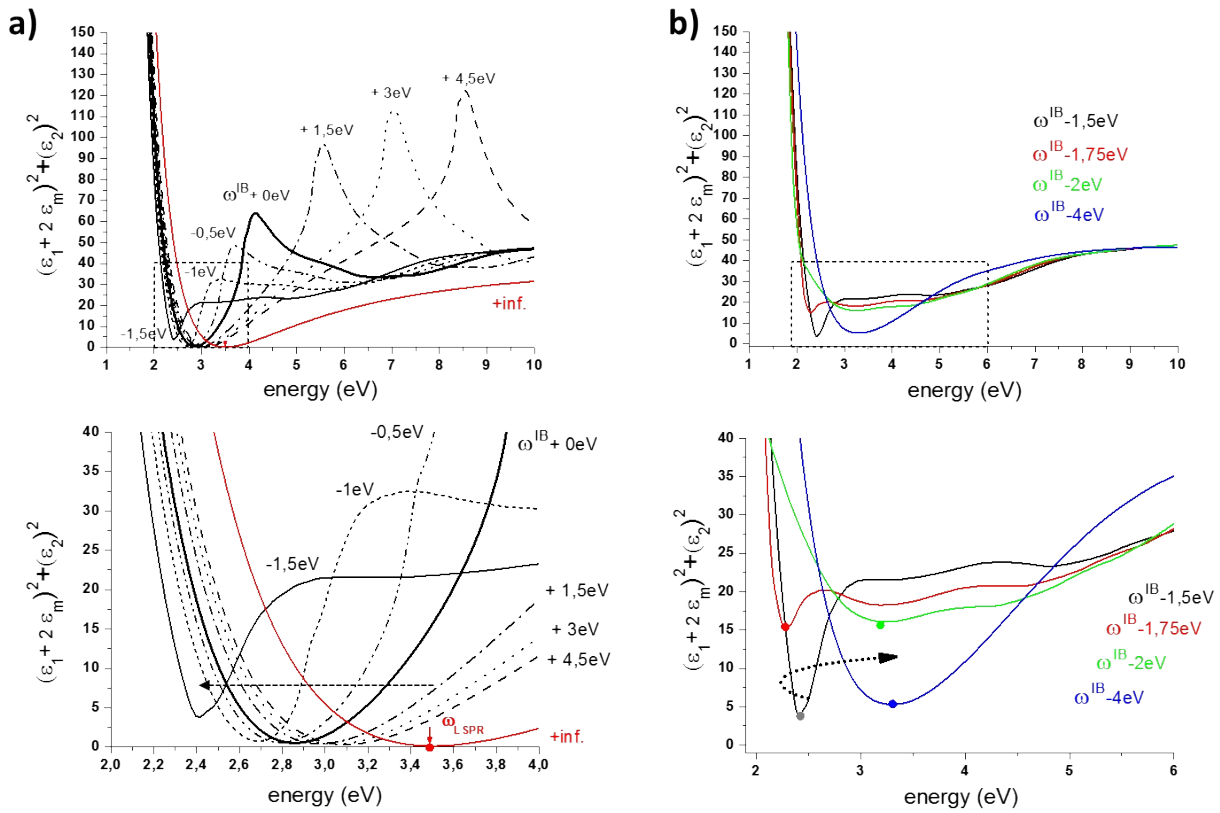

Figure SI4. Values of the absorption cross section denominator $(\varepsilon_1(\omega)+2\varepsilon_m)^2+\varepsilon_2(\omega)^2$ *for a silver metallic sphere as a function of various shifts artificially applied to the IB absorption threshold (from +4.5eV down to -1.5eV in (a), from -1.5eV down to -4eV in (b)).The lower*

figures give zoomed parts of the upper ones indicated by dotted line rectangles. The red curve (a) is obtained for a Drude metal (silver parameters with $\varepsilon_\infty = 1$*). A dielectric function* $\varepsilon_m = 2.7$ *is assumed for the outer dielectric medium.*

For an infinite positive offset (red curve in Figure SI4a), IB transitions are ignored and the Drude model is recovered. The denominator (SI4) is $1 - \frac{\omega_p^2}{(\omega^2 + \omega\Gamma^2)} + 2\varepsilon_m$ and the resonance condition is fulfilled for $\omega_{LSPR}^S = \frac{\omega_p}{\sqrt{1 + 2\varepsilon_m}}$ (red arrow in the lower panel of Fig. SI4a).

For IB threshold shifts δ ranging from 4.5ev down to -1eV, the curves present a minimum that progressively shifts towards low energies as compared to the Drude value. This is consistent with an expected red shift due the increasing effect of the dielectric screening by the ionic background (increasing value of $Re[\chi_{IB}(\omega)]$ in the expression of $\varepsilon_1(\omega)$) since all the minima are given by the zeros of $\varepsilon_1(\omega) + 2\varepsilon_m$ in a good approximation. It must be noted that the more the curve dips are sharp around their minimum the narrower will be the resonance peak in the absorption cross-section. As can be seen in Figure 1a of the main paper, this width remains constant for δ values down to -1eV. However, below this limit, the role of $Im[\chi_{IB}(\omega_R)]$ becomes critical and the profile of $(\varepsilon_1(\omega) + 2\varepsilon_m)^2 + \varepsilon_2(\omega)^2$ changes drastically. For $\delta = -1.5eV$, the minimum is always red-shifted but much sharper. This is also reflected in the LSPR peak in Figure 1a. Figure SI4b shows that below this value, the curve flattens and discloses secondary minima. The most pronounced of them is now blue-shifted with decreasing δ. Below $\approx -3eV$, the spectral dependence of $Im[\chi_{IB}(\omega)]$ is softer. A single minimum is detected but in a broad well which explains the large width of the LSPR resonances for $\delta = -3eV, -4eV$ in Figure 1a of the main text.

Generally speaking, this mechanism of a LSPR shift reversal can be explained by considering both the approximate resonance condition $\varepsilon_1(\omega_R^S) + 2\varepsilon_m = 1 - \frac{\omega_p^2}{\omega_R^{S2} + \Gamma^2} + Re[\chi_{IB}(\omega_R^S)] + 2\varepsilon_m = 0$ and the dispersive profile of $Re[\chi_{IB}(\omega)]$ that is swept over the LSPR as the IB absorption continuum threshold is red-shifted (see Figure SI1)

The same analysis is difficult to carry out in the case of the nanoshell where both the numerator and denominator spectral variations have to be considered in the expression of the absorption cross-section (SI8). However, similar mechanisms would govern the evolution of the high energy resonance (ω_+) of the nano-shell (see Figure 1b)

4 LSPR of nickel nanosphere and nanoshell

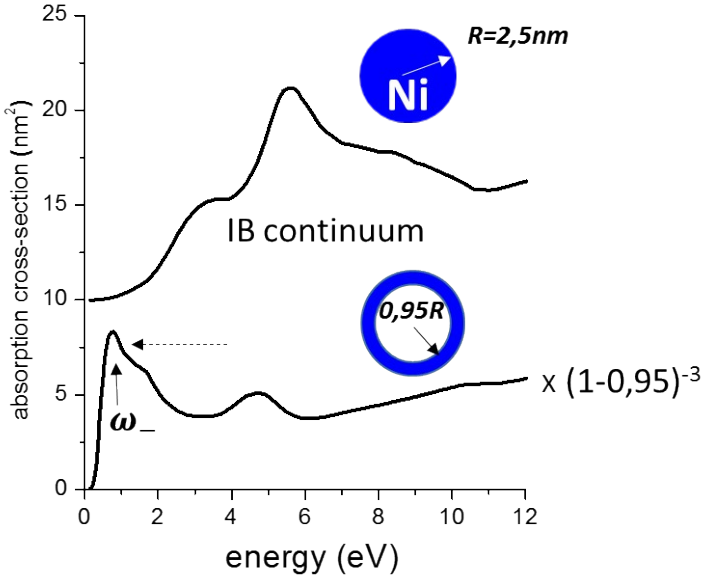

Figure SI5. Optical absorption spectra of a nickel nanosphere (upper curve) and a nickel nanoshell with a 5% relative shell thickness (lower curve). The dielectric function of nickel has been taken from Palik tables [3]. Those of the inner dielectric core and the surrounding medium are assumed to have the common value $\varepsilon_m = 2.7$ *. The magnitude of the lower curve has been corrected to account for the proportionality of the absorption signals with the metal volume. The upper curve has been offset vertically by 10 nm². In the case of the nanoshell, the maximum absorption peak at 1 eV is not a structure of the IB continuum but the signature of the red-shifted low energy resonance of the shell (*ω_-*). The high energy resonance (*ω_+*) is damped in the absorption continuum.*

5 Real and imaginary parts of the polarizability of a silver nanosphere in the dipolar approximation.

The polarizability of a spherical particle with radius R (R<<c/ω) embedded in a medium of constant dielectric function ε_m writes

$$\alpha^S(\omega) = 3\left(\frac{4}{3}\pi R^3\right)\frac{(\varepsilon(\omega)-\varepsilon_m)}{(\varepsilon(\omega)+2\varepsilon_m)}$$

Figure SI6 shows the real and imaginary parts of this polarizability for a silver sphere of dielectric function $\varepsilon(\omega)$ including IB transitions (experimental dielectric function) or not including IB transitions (Drude approximation).($\varepsilon_m = 2.7, \varepsilon_\infty = 1$).

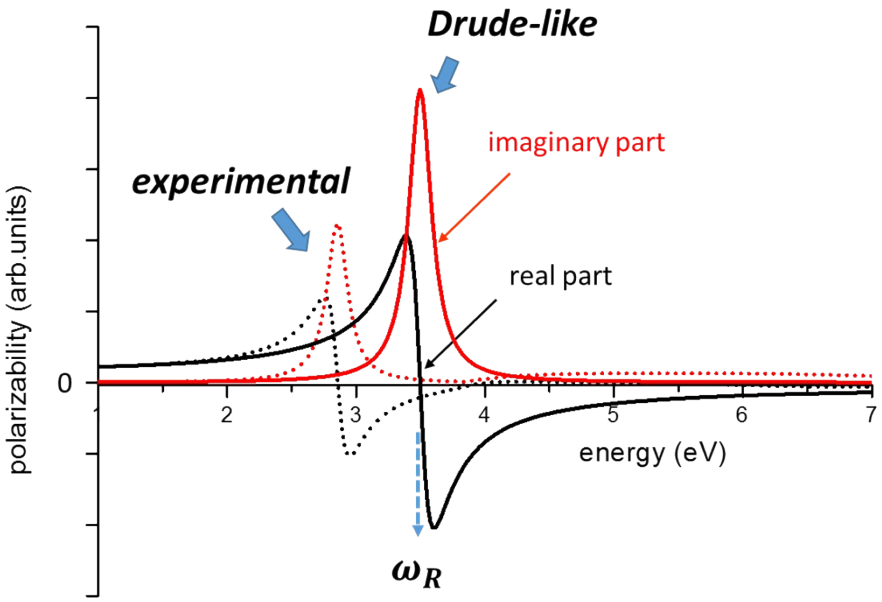

Figure SI6 Real (black) and imaginary (red) parts of a silver nanosphere polarizability in the dipolar approximation. The full line curves are obtained assuming a pure Drude dielectric function (see the parameters ω_p^{Ag}, Γ^{Ag} in Table SI1).The dotted line curves correspond to the experimental dielectric function of silver. [3]

The real part of the polarizability changes sign across the plasmon resonance ω_R and then the phase of the oscillating particle dipole will experience a π phase shift relative to the applied electric field.

6 Compared optical responses of Au@Cu and Cu@Au core-shell nanoparticles

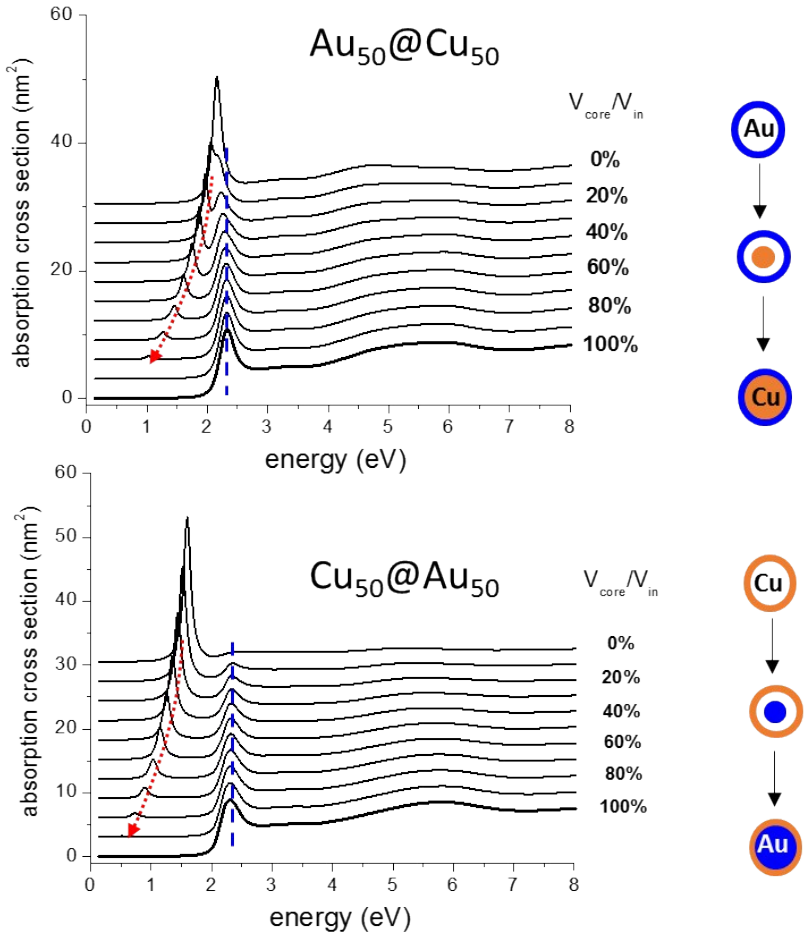

Figure SI7. Comparison between the calculated optical absorptions of Au@Cu and Cu@Au core-shell clusters (r_{out}=2.5nm). V_{core}/V_{in} defines the filling of the inner volume by the growing core from the single shell to the full core-shell structure from the top to the bottom. Shell thicknesses are set by assuming a 50%-50% atomic composition for the final structure (about 0.4nm for Au@Cu and 0.64nm for Cu@Au). The shift of the hybridized level originating from the single shell low energy resonance (ω_-) is indicated by red dotted arrows. Vertical blue dotted lines show the emergence of the high-energy resonance of the core-shell system (at the contact limit) that originates from the LSPR of the growing spherical core. A common real dielectric function $\varepsilon_m = 2.7$ is assumed for inner and outer dielectric media.

7 Compared optical response of Cu@Ag and Ag@Cu nanoparticles: core/shell coupling and composition effects from the Mie theory.

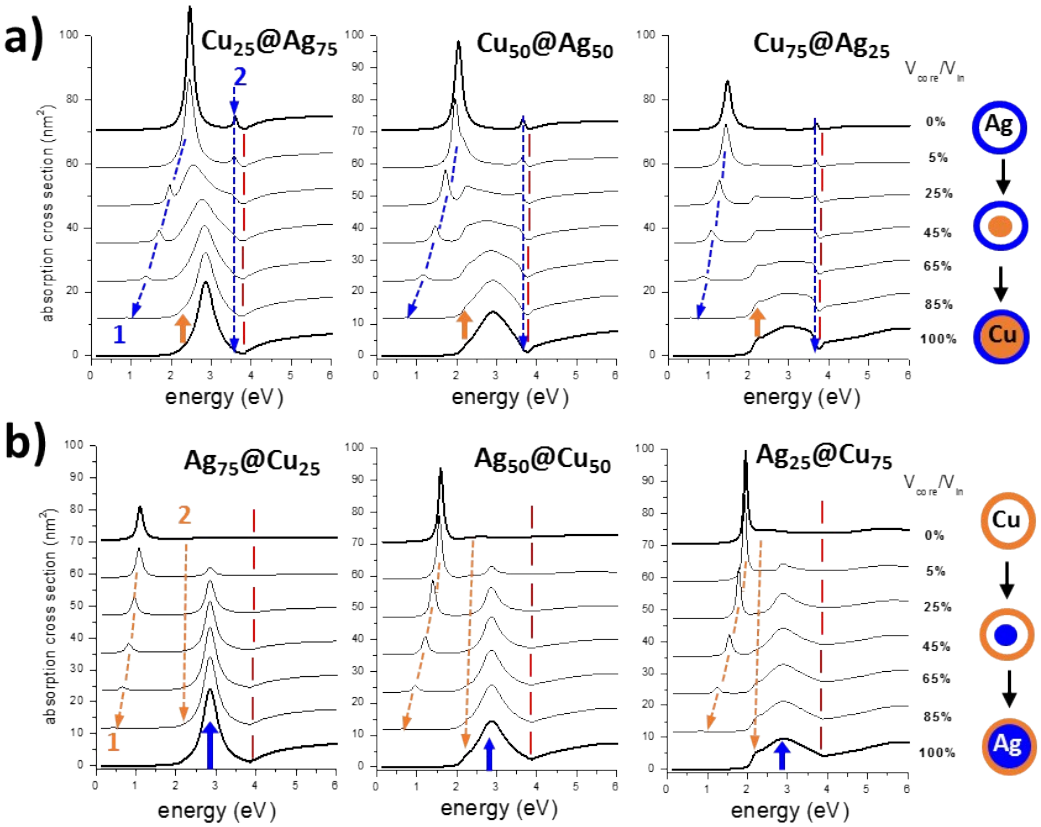

Figure SI8. (a) Calculated optical absorption of Cu@Ag core-shell clusters of radius r_{out}=2.5nm. V_{core}/V_{in} is the filling factor of the inner volume by the growing core, from the single shell to the full core-shell structure. Shell thicknesses are set from the respective atomic compositions indicated at the top of the figure for the final structures where V_{core}/V_{in}=100%. The blue dotted lines show the spectral shifts of the low energy shell resonance (1) that vanishes at the core-shell contact and of the high energy resonance (2). The orange arrow locates the pure copper core resonance at the onset of the copper IB absorption continuum. The "Fano dips" induced by the high energy silver shell resonance (2) are marked by red bars.

(b) Identical calculations made for inverted Ag@Cu structures. The color code (orange/blue) is also inverted. The orange dotted lines show the spectral shift of the low energy shell resonance that vanishes at the core-shell contact (1) and the position of the damped high energy shell resonance (2) that couples with the growing silver core (blue arrow). The same dielectric function $\varepsilon_m = 2.7$ is assumed for inner and outer dielectric media.

8 Compared optical response of Ni@Ag and Ni@Au core/shell nanoparticles from Mie theory calculations.

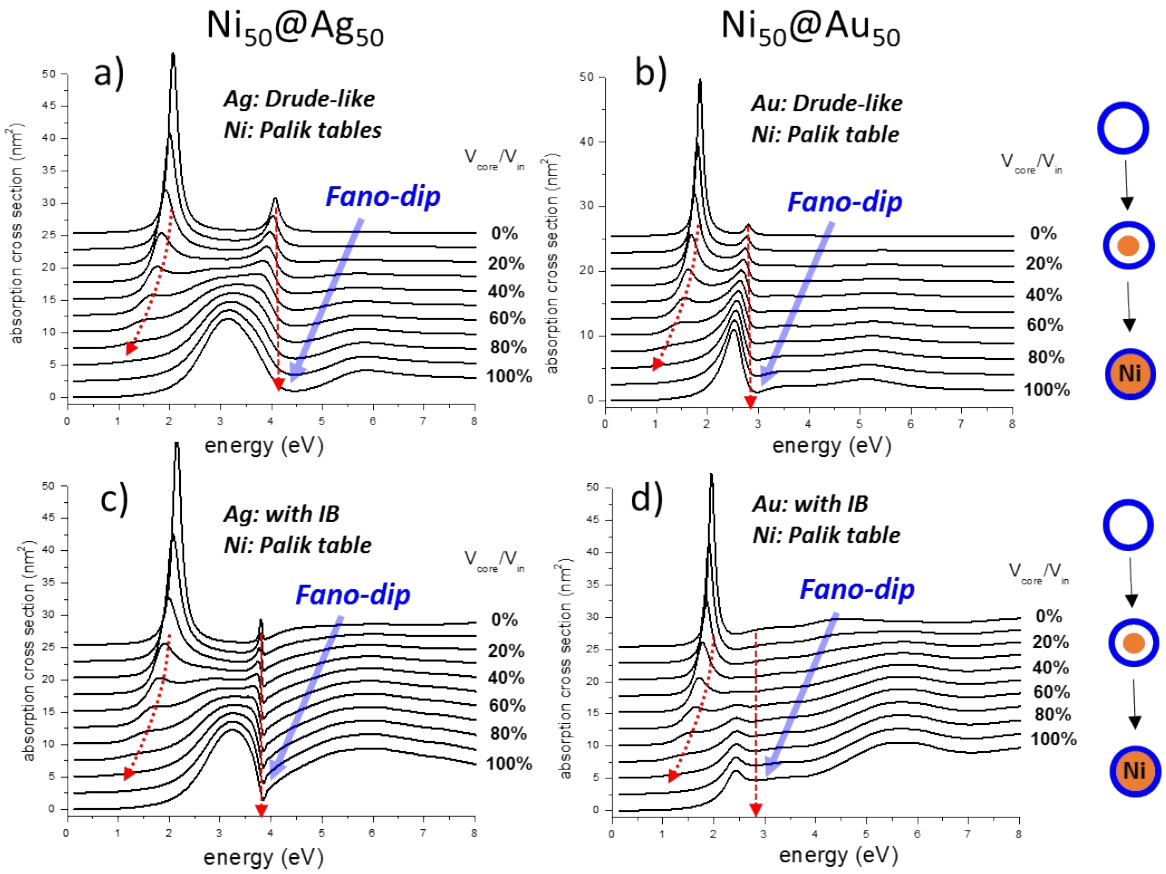

Figure SI9: Comparison between the optical absorption of Ni@Ag (left) and Ni@Au (right) core-shell clusters (outer radius r_{out}=2.5nm). V_{core}/V_{in} defines the filling of the inner volume by the growing core from the single shell to the full core-shell structure from top to bottom. Both shell thicknesses are defined by assuming a 50%-50% atomic composition for the final core-shell structure (V_{core}/V_{in}=100%). Upper figures (a) and (b) are obtained for Drude-like silver ignoring IB absorption continuum. Lower figures (c) and (d) assume the full dielectric constant of silver. The dielectric constant of nickel includes IB polarizability.[3] The shifts of hybridized levels originating from single shell (ω_- and ω_+) resonances are indicated by red dotted arrows. The so-called "Fano dips" result from the interaction of the high energy shell resonances (ω_+) with the nickel absorption continuum. The same real dielectric function $\varepsilon_m = 2.7$ is assumed for inner and outer dielectric media.

REFERENCES

(1) Lermé, J.; Palpant, B.; Prével, B.; Cottancin, E.; Pellarin, M.; Treilleux, M.; Vialle, J. L.; Pérez, A.; Broyer, M. Optical properties of gold metal clusters: A time-dependent local-density-approximation investigation. *European Physical Journal D* **1998,** *4*, 95-108.

(2) Cottancin, E.; Langlois, C.; Lermé, J.; Broyer, M.; Lebeault, M. A.; Pellarin, M. Plasmon spectroscopy of small indium-silver clusters: monitoring the indium shell oxidation. *Physical Chemistry Chemical Physics* **2014,** *16*, 5763-5773.

(3) Palik, E. D., *Handbook of optical constants of solids*. Academic Press: New York, 1991.

(4) Bohren, C. F.; Huffman, D. P., *Absorption and Scattering of Light by Small Particles*. Wiley: New York, 1983.

(5) Hodak, J. H.; Henglein, A.; Giersig, M.; Hartland, G. V. Laser-induced inter-diffusion in AuAg core-shell nanoparticles. *Journal of Physical Chemistry B* **2000,** *104*, 11708-11718.